Received: 17.06.2024 *Accepted: 16.07.2024* *Published: 02.08.2024*

Understanding Damage Initiation and Propagation Mechanisms in Polyurethane Foam Core Sandwich Panels Using Acoustic Emission Monitoring

[1]Chouiter Adel, [2]Keskes Boualem, [3]Benzerga Djebbara, [3]Reffas Sid Ahmed, [3]Habib Berrekia

[1]University Frères Mentouri Constantine 1, BP, 325 Ain El Bey, 25017 Constantine, Algéria,
adel.chouiter@umc.edu.dz https://orcid.org/0009-0003-1064-1805
[2]University Farhat Abbas Sétif, Campus El Bez. Sétif 19137, Algéria.
bkeskes2012@gmail.com https://orcid.org/0009-0007-1100-8875
[3]University of Sciences and Technology of Oran, Mechanical Department, B.P. 1505, 31000 Oran, Algeria.
djebbara.benzerga@univ-usto.dz https://orcid.org/0000-0003-2238-6488
reffas_ahmed@yahoo.fr https://orcid.org/0009-0005-4879-3884
habib.berrekia@univ-usto.dz https://orcid.org/0000-0002-9569-0520

Abstract
Comprehending the damage initiation and propagation mechanisms in sandwich materials is crucial for optimizing their design. We employ a passive approach based on three-point bending tests on prismatic sandwich beam specimens with polyurethane foam cores. During these tests, the acoustic emission (AE) signals generated by the materials under mechanical loading are recorded. AE is defined as the release of energy in the form of transient elastic waves accompanying a dissipative process in the material. These signals are then analyzed based on parameters such as amplitude, energy and number of events to study the influence of support span length and core thickness. Classification of the acoustic signatures allows identification of the different damage modes (core shear, delamination, indentation, etc.). This acoustic activity is correlated with the deformation phases (load-displacement curve) and the damage modes observed in real-time. This correlation enables evaluation of the collected signals and improves understanding of the damage mechanisms in sandwich materials.

Keywords: Sandwich panels, polyurethane foam, three-point bending, acoustic emission, damage modes.

1. Introduction

In recent years, growing interest has focused on developing and characterizing new sandwich panel configurations using innovative materials and manufacturing techniques. Limited research exists on the flexural behavior and damage mechanisms of these sandwich panels, especially using advanced monitoring techniques like acoustic emission.

These materials are experiencing remarkable growth in various industrial sectors, notably aerospace, automotive and construction, composed of two thin skins bonded to a lightweight core due to their excellent strength-to-weight ratio, stiffness and insulation properties [1].

The skins provide high in-plane strength and stiffness, while the core material separates the skins and resists shear loads. Foam materials, such as polyurethane, polyethylene and phenolic foams, are commonly used as core materials in sandwich panels due to their low density, good mechanical properties and ease of manufacturing, Yan and al. [2]. However, the complex nature of sandwich structures, combining different materials and interfaces, makes their mechanical behavior and damage modes difficult to predict [3]. In particular, the flexural behavior of these structures is crucial for many applications but remains insufficiently understood, especially regarding damage initiation and propagation by Carlsson and al [4].

Recent research has highlighted the importance of understanding the mechanical behavior of sandwich structures under various conditions. For example, Monteiro and al [5] studied the effect of dimensions and relative density on the mechanical behavior of lattice core cellular structures manufactured by additive manufacturing for sandwich panels. Their results showed that the core geometry and density significantly impact the overall mechanical properties of the sandwich. In the field of sports applications. Crameri and al. [6] conducted an experimental study on the mechanical performance of EPS foam core sandwich composites used in

surfboard design. This study emphasized the importance of material selection and structural design for optimizing the performance of sports equipment. Regarding metallic sandwich structures. Huang, et al. [7] examined the effect of core density on the three-point bending performance of aluminum foam core sandwich panels. Their work underlined the importance of core density in determining the failure modes and overall mechanical properties of sandwich panels.

In this context, acoustic emission (AE) refers to the transient elastic waves generated by the rapid release of energy from localized sources in materials undergoing deformation or damage by Grosse and al. [8].

Saeedifar and al. [9] Used acoustic emission (AE) as a non-destructive testing technique for real-time monitoring and damage assessment in composite materials and structures. Fotouhi and al. [10] detected and analyzed AE signals using piezoelectric sensors, obtaining valuable information about the type, location and severity of damage in the material. Assarar and al. [11] contributed to identifying the damage mechanisms created in sandwich composites (glass fiber-polyvinyl chloride (PVC)) subjected to three-point bending tests. To optimize the investigation of damage mechanisms, the recorded AE signals are classified using multivariate data analysis, where the mechanisms are tracked until the failure of the tested samples. Pyrzowski and al. [12] integrated two diagnostic techniques (acoustic emission and digital image correlation) to improve damage assessment during the mechanical degradation process. The results showed that both techniques allowed observing the folding process as well as classifying the damage stages. Ben Ammar and al. [13] studied the mechanical behavior of sandwich structures under static and dynamic 4-point bending tests. The effects of foam and density on the static and fatigue mechanical behavior were investigated using acoustic emission to identify and characterize local damage. Leone and al. [14] evaluated the initiation, progression of damage and anticipation of fracture in a notched honeycomb. The results were correlated with photogrammetric strain fields and acoustic emission for detecting damage initiation at the notch and tracking the progression until final failure.

The present study aims to examine the three-point bending behavior and damage mechanisms of sandwich panels with polyurethane foam cores and steel skins, manufactured by the company HODNA METAL, using acoustic emission monitoring. The objectives are to identify and classify the different damage modes occurring during three-point bending tests and correlate the AE parameters with the damage events. Eventually, the flexural behavior and AE are compared for different sample configurations and loading conditions.

This research is part of an approach to optimize sandwich structures for local industrial applications by providing valuable information on their mechanical behavior and damage mechanisms. The results of this study can contribute to improving the design and use of these materials in various industrial sectors and beyond.

2. Materials and experimental procedure

2.1 Materials

The company HODNA METAL provided the sandwich panels studied. They are intended for various cladding applications (cold rooms, industrial buildings, etc.). The structure of this type of sandwich consists of a rigid polyurethane foam core and S250 steel skins [15]. The mechanical properties of the core and skins are presented in Tables 1 and 2 respectively.

Table 1: Mechanical properties of the polyurethane foam core [15].

Property (polyurethane foam)	values	
Elastic modulus	2409	MPa
Shear modulus	862.2	MPa
Density	40	kg/m³
Tensile strength	40	MPa
Thermal conductivity	0.022	W/m.°C

Table 2: Core Mechanical properties of S250 steel skins [15].

Property of steel	values	
Elastic modulus	2^{e}+05	MPa
Shear modulus	7.93^{e}+ 05	MPa
Density	7850	kg/m³
Tensile strength	400	MPa
Yield strength	250	MPa

2.2 Specimen preparation

The specimens were cut into different geometric configurations by varying the support span (L) and core thickness (h), as detailed in Table 3.

Table 3: Dimensions of specimens used for three-point bending tests.

L (mm)	b (mm)	h (mm)	t_c (mm)	t_f (mm)
80	40	30	28.6	0.70
		100	98.6	
100	40	30	28.6	0.70
		100	98.6	
120	40	30	28.6	0.70
		100	98.6	
200	40	30	28.6	0.70
		100	98.6	
300	40	30	28.6	0.70
		100	98.6	
400	40	30	28.6	0.70
		100	98.6	
500	40	30	28.6	0.70
		100	98.6	

Where L is the distance between supports, b the width of the specimen, h the total thickness, tc the thickness of the core and tf the thickness of the skins.

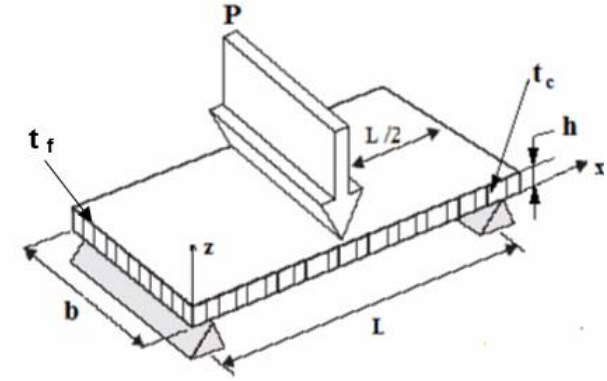

Figure 1: Geometric characteristics of a sandwich panel.

2.3 Experimental procedure

2.3.1 Three- point bending tests:

The three-point bending tests were carried out on a Zwick/Roell tension-compression machine equipped with a 100 kN load cell, in accordance with the ASTM C393-62 standard. The tests were performed at loading rates of 2 and 5 mm/min. A flexure fixture adapted to the machine was used to allow varying the support span. The specimens are placed on the bending device with variable support spans (100, 200, 300, 400mm) (Figure 2) adaptable to the tensile machine.

Figure 2: The three-point bending device on the Zwick/Roell traction machine.

2.3.2 Acoustic emission monitoring:

Damage monitoring was performed using an acoustic emission chain consisting of two piezoelectric sensors (VS 45H) with preamplifiers and an AMSYS-6 acquisition system. The sensors, with a resonance frequency of 275 kHz, were positioned on the surface of the specimens using silicone grease and held in place with adhesive tape. The signals were amplified with a gain of 34 dB and an acquisition threshold of 34 dBEA.

The settings and characteristics of the instrumentation are detailed below:

✓ Acquisition system - Number of channels: AMSYS - 6

✓ Number of channels used for the examination: 2
✓ Sensor type - Number: VS 45H - 2
✓ Resonant frequency (kHz): 275 kHz
✓ Preamplifiers (AEP4): with Gain (dB): 34
✓ Acquisition threshold (dBEA: Ref. 1 µVolt/Sensor): 34

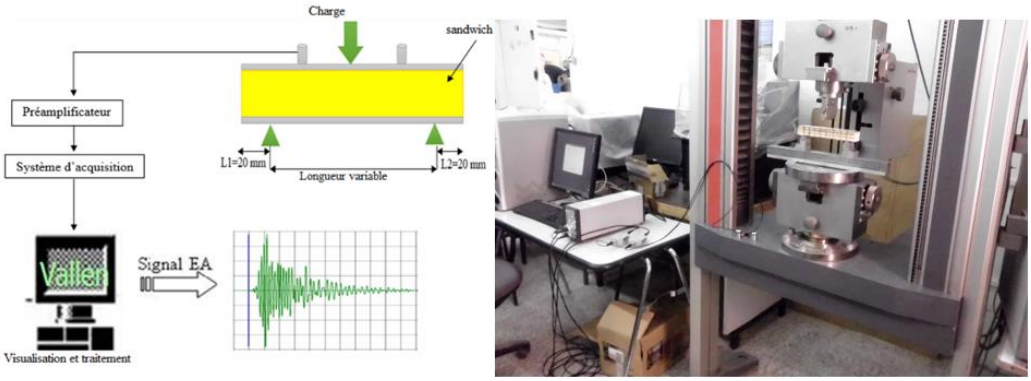

Figure 3: Principle and overview of the acoustic emission device.

3. Results and Analysis

3.1 Mechanical behavior in three-point bending and discussion

3.1.1 Effect of Support Span:

The Load-deflection curves obtained for different support spans are presented in Figure 4.

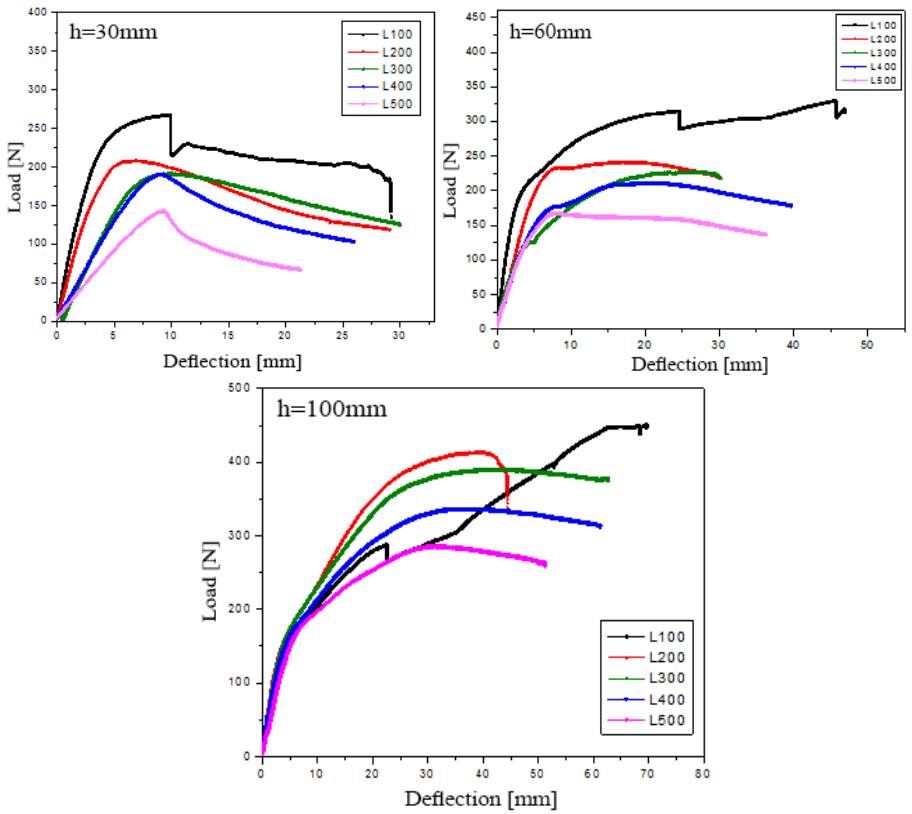

Figure 4: Load-deflection curves for different distances between supports (h = 30 mm, h = 60mm, h = 100mm).

3.1.2 Effect of Sandwich Core Thickness:

Figure 5 illustrates the effect of different thicknesses on the flexural behavior of the sandwich panels.

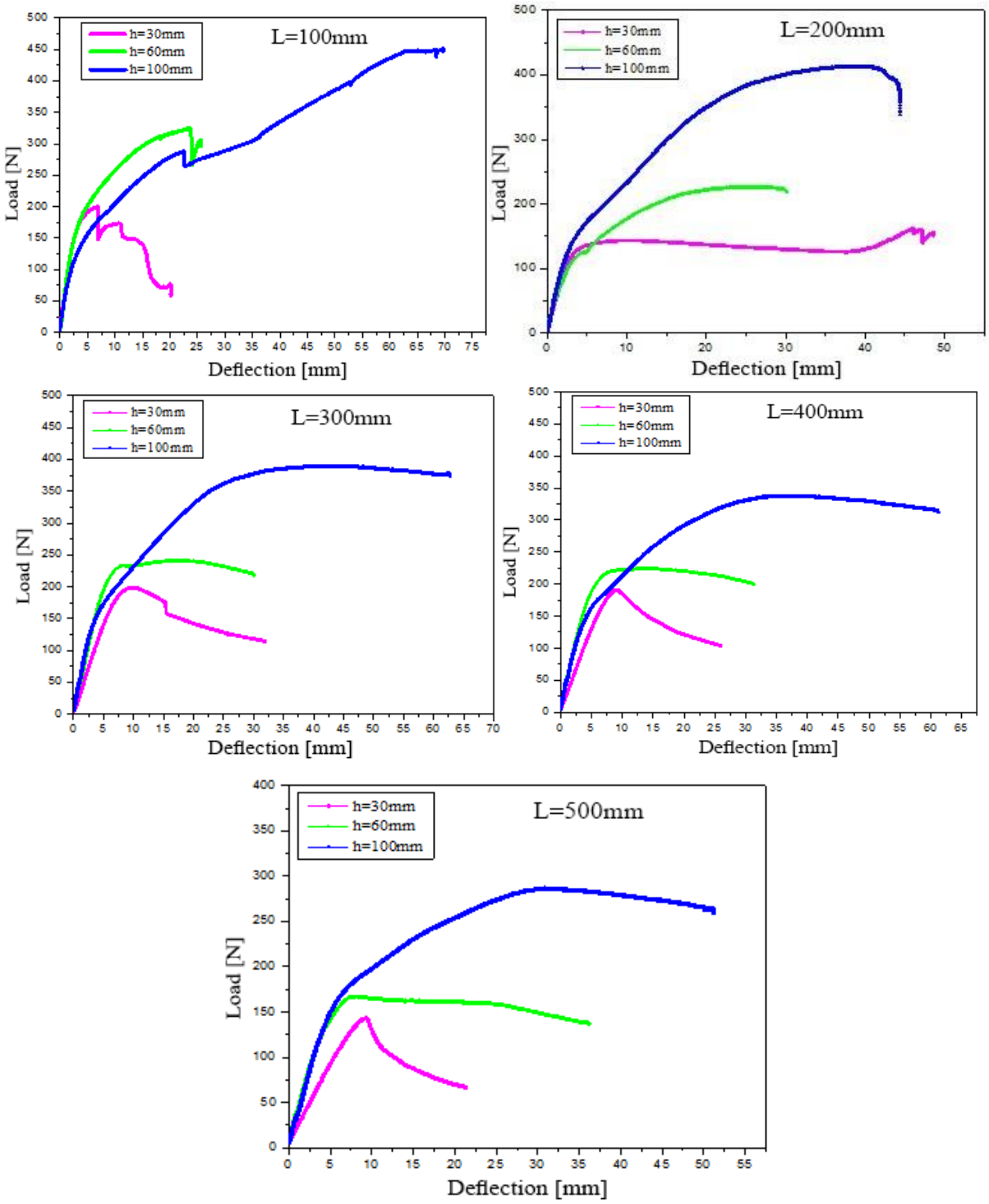

Figure 5: Load-deflection curves for (L=100mm, L=200mm, L=300mm, L=400mm, L=500 mm) for different core thicknesses.

It is observed that the flexural behavior of the sandwich panels can be divided into three distinct phases:

a. An initial linear phase, corresponding to the skins working in tension/compression.
b. A second nonlinear phase, associated with the shear strength supported by the core.
c. A third phase: rupture phase characterized by the decrease in force.

(Figure 4) The analysis of these curves reveals that the maximum load and flexural stiffness decrease with increasing support span. This phenomenon can be attributed to the increase in bending moment and the reduction in the influence of transverse shear for larger support spans.

(Figure 5) It is found that the maximum load and flexural stiffness increase with core thickness. This trend is explained by the increase in the section's moment of inertia and the core's shear strength with thickness.

3.2 Results and Analysis of Acoustic Emission Signals

The analysis of the AE data focused on three main parameters:
1. The number of events (hits).
2. The maximum amplitude of the hits (in dB).
3. The energy of the hits (in arbitrary units).
These parameters were studied as a function of the variation in support span, core thickness and loading rate. Temporal and frequency analysis of the signals was performed to identify the acoustic signatures corresponding to the different damage modes.

3.2.1 Acoustic emission result of the foam core:

A bending test was performed on a foam specimen with a section of 30 cm × 10 cm. Two piezoelectric sensors were placed on the front and back faces of the panel.
The purpose of this test is to determine the acoustic signature of the source mechanism corresponding to the evolution of damage within the core. Figures (6.1-6.2-6.3-6.4) represent the load-deflection curves with monitoring of the acoustic activity during the bending test. The acoustic activity is represented by the number of cumulative hits, maximum amplitude (dB) and cumulative energy as a function of time.

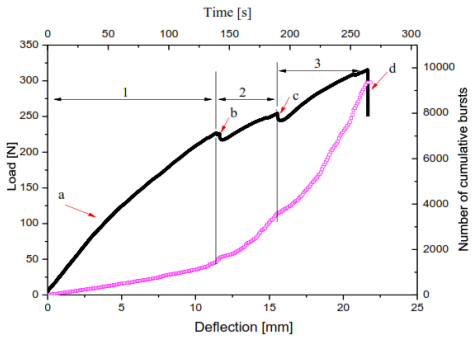

Figure 6.1: Load-deflection curve and number of cumulative bursts as a function of time.

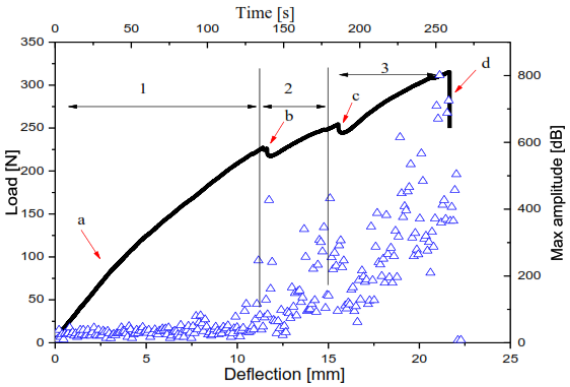

Figure 6.2: Load-deflection curve and Max amplitude (dB) of bursts as a function of time.

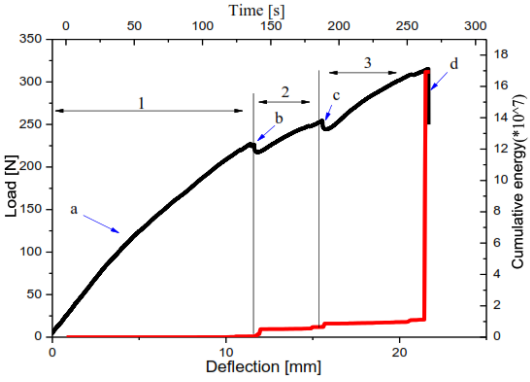

Figure 6.3: Load-deflection curve and cumulative energy as a function of time.

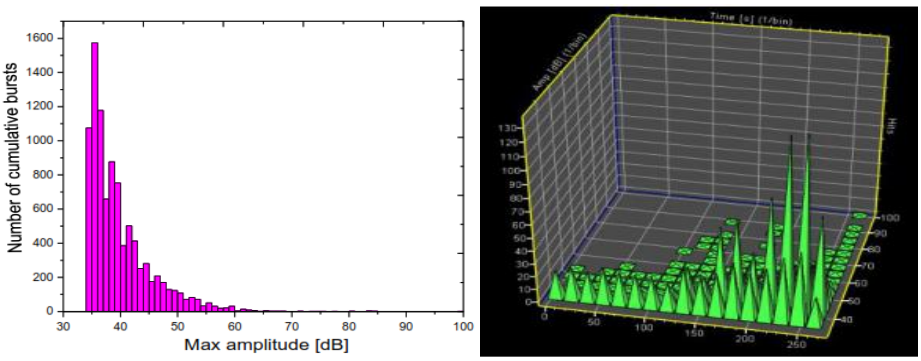

(a) **(b)**

Figure 6.4: Amplitude distribution (a) and the evolution over time of the amplitude distribution in the foam core (b).

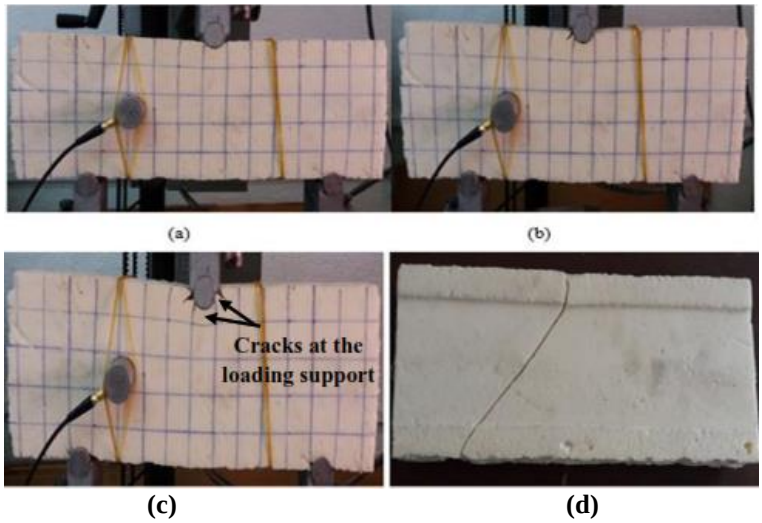

Figure 7: The timeline of the damage to the foam board.

The acoustic monitoring of the damage to the foam panel shows the existence of three different phases (Figures 6.1-6.2)

1) The first phase corresponds to the classic behavior of foams, a linear behavior up to a deformation of 12%, this phase is characterized by low amplitude and energy signals; the number of hits increases regularly.

2) The second phase: the foam is strongly indented at the contact with the loading support; the high penetration of the latter leads to the creation of cracks around the loading support (Figure 7.b and 7.c). At this stage, the acoustic activity becomes relatively important.

3) The third phase: the propagation of these cracks leads to a very high acoustic activity (the number of hits reaches 112, an amplitude of 70dB and an energy of about 17×10^7 eu) causing a transverse shear damage mode leading to the final failure of the panel (Figure 7.c).

The drops observed in the load-displacement curve are due to the cracking of the panel at the loading point: the drop (b) corresponds to the first observed cracking (Figure 7.b), the appearance of a second crack on the other side of the loading point causes another drop observed at point (c) (Figure 7.c), while the last drop (point d) corresponds to shear or total cracking along the thickness of the panel (Figure 7.d).
The analysis of the amplitude distribution of the acoustic emission hits allowed classifying the amplitude range of 35-65dB corresponding to the damage mode by shearing of the foam.

3.2.2 Acoustic emission result of the steel skin:
A tensile test was performed on a steel specimen with a section of $200\times25\times0.7$ cm^3. Two sensors were placed on the specimen (Figure 8).

Figure 8: Tensile test of the steel skin.

The purpose of this test is to determine the acoustic signature of the source mechanism corresponding to the evolution of damage in the skins.

Figures (9.1-2-3-4) show the load-elongation curves with monitoring of the acoustic activity during the skin tensile test. The acoustic activity is represented by the number of cumulative hits, cumulative energy and maximum amplitude (dB) as a function of time.

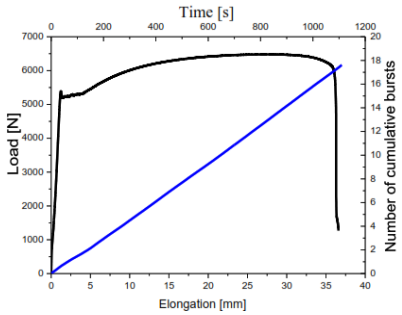

Figure 9.1: Load-elongation curve and number of cumulative bursts as a function of time.

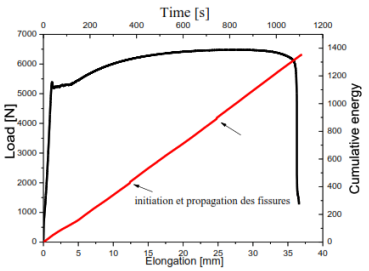

Figure 9.2: Load-elongation curve and cumulative energy as a function of time.

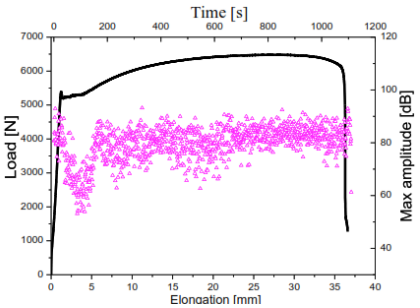

Figure 9.3: Load-elongation curve and Max amplitude (dB) of bursts as a function of time.

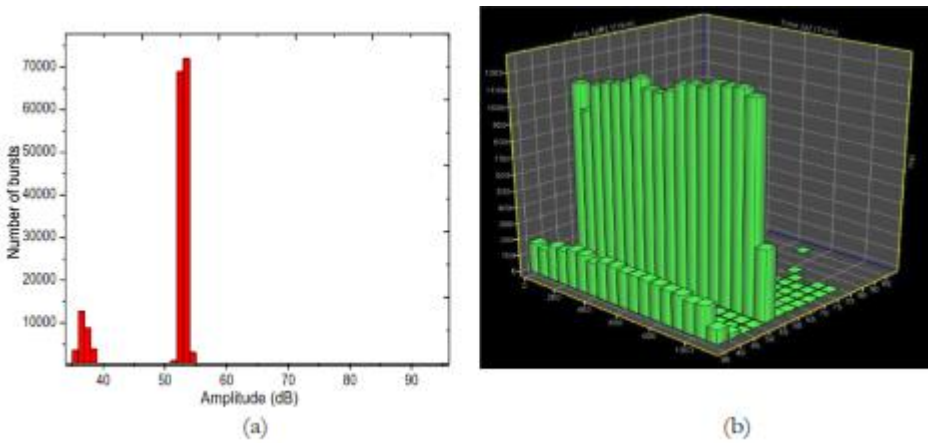

Figure 9.4: Amplitude distribution (a) and the evolution of the amplitude distribution as a function of time in the skin of the sandwich (b).

The analysis of the obtained acoustic emission results shows three domains of activity such as:

1. In the elastic domain of the load-elongation curve, the acoustic emission is important which can be due to emissive mechanisms such as the tensioning of the specimen.
The acoustic emission is important at the elastic limit and then progressively decreases as the deformation increases.

2. For larger elongations (very large plastic domain), a more discontinuous activity is noted due to the plastic deformation of the skin.

3. A zone generating very dense acoustic emission due to the failure that occurs by necking.

The evolution of the number of cumulative hits and cumulative energy for steel is regular (linear).
The analysis of the amplitude distribution of the acoustic emission hits allowed classifying the amplitude range of 35-55dB corresponding to the damage mode by plastic deformation of the skin.

3.2.3 The effect of support span and core thickness:

The curves of cumulative hits and energy for different support lengths (80, 100, 120mm) and thicknesses (30, 100mm) are illustrated by figures (10.1-2-3-4-5-6).

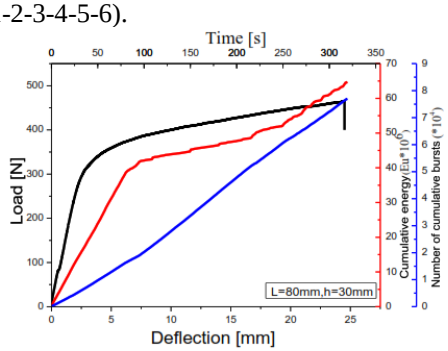

Figure 10.1: The charge-deflection curve and the evolution of bursts and cumulative energy for L=80mm and h=30mm.

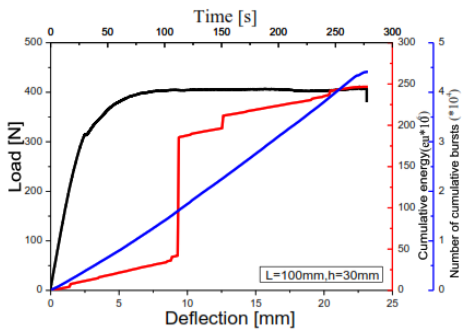

Figure 10.2: The charge-deflection curve and the evolution of bursts and cumulative energy for L=100mm and h=30mm.

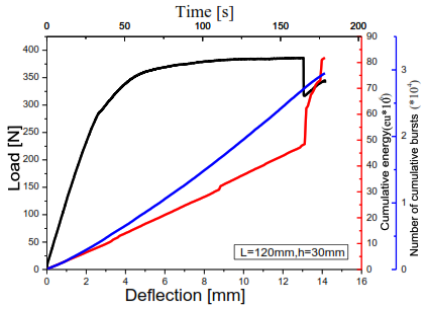

Figure 10.3: the charge-deflection curve and the evolution of bursts and cumulative energy for L=120mm and h=30mm.

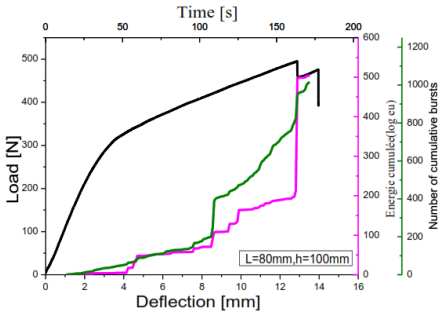

Figure 10.4: the charge-deflection curve and the evolution of bursts and cumulative energy for L=80mm and h=100mm.

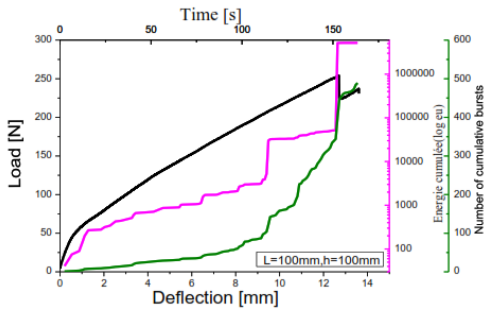

Figure 10.5: the charge-deflection curve and the evolution of bursts and cumulative energy for L=100mm and h=100mm.

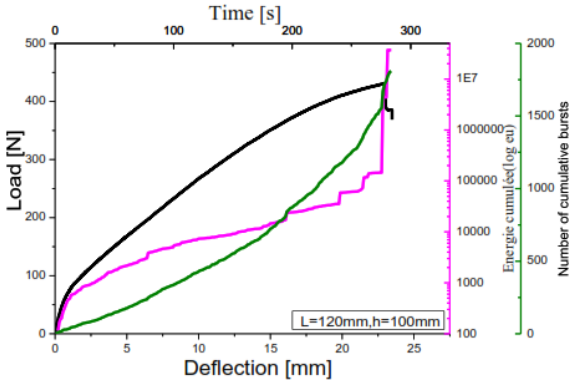

Figure 10.6: The charge-deflection curve and the evolution of bursts and cumulative energy for L=120mm and h=100mm.

From the various results obtained, it can be seen that the load-displacement test curves and those of the acoustic emission can be divided into three phases:

(1) Phase 1: which characterizes the elastic behavior of the sandwich structure. This phase is described by low acoustic activity.
(2) Phase 2: characterizes the plastic behavior of the sandwich structure, this phase is described by high acoustic activity following the initiation of several micro cracks.
(3) Phase 3: characterizes the failure by indentation, core shear and skin-core delamination, a very high acoustic emission is observed in this phase.
The characteristics of the acoustic emission signals of each damage mode observed on the specimens for different support spans and core thicknesses are presented in the table 4 below:

Table 4: Characteristics of the acoustic emission signals for different distances between supports and thicknesses of the core.

Thickness (mm)	Distance between supports (mm)	Mode of damage	Amplitude (dB)	Energy (EU)	Number of bursts
h=30	L=80	Core/skin delamination	35-60	$4.07*10^5$	220
	L=100	Localized indentation	35-55	$4.75*10^6$	197
	L=120	The core shear	35-65	$7.98*10^6$	162
h=100	L=80	The core shear	35-50	$2.8*10^5$	127
	L=100			$5.13*10^6$	56
	L=120			$3.26*10^7$	29

✓ For the specimens of thickness h=30mm, the damage mode differs from one length to another which are respectively:

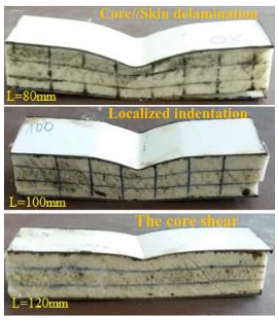

Figure 11: Damage modes for specimens with a thickness of h=30mm.

✓ For the specimens of thickness h=100mm the damage mode is unique which is the core shear

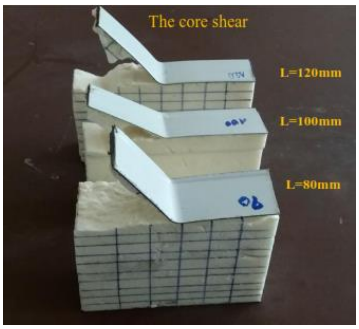

Figure 12: Mode of damage to specimens with thickness h=100mm.

✓ For each thickness, the increase in the support length leads to an increase in the energy released and a decrease in the number of hits.
✓ For the same support length and different core thicknesses presenting the same damage mode (L=120mm specimen), it can be seen that the energy increases and the number of hits decreases with increasing thickness (h=30,100mm).

4. Thorough Discussion of Results

4.1 Observed Failure Modes

The main failure modes identified in the study are:

✓ Core shear: This failure mode is mainly observed for shorter support spans and larger core thicknesses. It is characterized by significant deformation of the foam core under the effect of shear forces, leading to a clean break.
✓ Localized Indentation: This failure mode occurs when the applied load is concentrated at one point, causing localized deformation of the foam core. This phenomenon is more frequent for intermediate support spans.
✓ Delamination between the core and the skin: This failure mode is characterized by a separation between the steel skins and the foam core, often observed for shorter support spans.

✓ Plastic Deformation of the Skins: This failure mode manifests as permanent deformation of the steel skins under the effect of the applied load.

4.2 Influence of Geometric Parameters

The study showed that:

The maximum load and flexural stiffness decrease with increasing support span. This is explained by the increase in bending moment for larger spans, thus reducing the structure's ability to withstand applied loads.

The maximum load and stiffness increase with core thickness. A thicker core provides better shear resistance, thus increasing the structure's ability to support higher loads.

For thin specimens (h = 30 mm), the failure mode varies according to the support span: delamination for short spans, indentation for intermediate spans, and core shear for long spans. For thick specimens (h = 100 mm), core shear is predominant regardless of the support span. These results underscore the crucial importance of geometry in the mechanical behavior of sandwiches.

4.3 Correlation between Mechanical Behavior and Acoustic Activity

The analysis of the acoustic emission signals allowed identifying three distinct phases:

✓ Elastic phase: Low acoustic activity, corresponding to the elastic behavior of the structure.
✓ Plastic phase: Strong increase in acoustic activity due to the initiation of microcracks.
✓ Failure phase: Very high acoustic activity, coinciding with the final failure of the specimen.

4.4 Acoustic Signatures of Damage Modes

The study made it possible to associate specific amplitude ranges with each damage mode:

✓ Core shear: 35-65 dB.
✓ Delamination: 50-56 dB.
✓ Localized indentation: 35-55 dB.
✓ Plastic deformation of the skins: 35-55 dB.

These results provide a basis for the non-destructive identification of damage modes in in-service sandwich structures.

5. Conclusion

This study analyzed the flexural behavior and damage mechanisms of sandwich panels with polyurethane foam cores and steel skins using the acoustic emission technique. The main conclusions are:

The maximum load and flexural stiffness decrease with increasing support span and increase with core thickness.

Four main damage modes were identified and characterized by their acoustic signatures: core shear, delamination, localized indentation and plastic deformation of the skins.

The geometry of the panels (support span and core thickness) significantly influences the dominant damage mechanisms.

The analysis of the acoustic activity allows monitoring the evolution of damage and correlating it with the mechanical behavior of the panels.

These results provide valuable information for optimizing the design and use of sandwich panels in various industrial applications.

REFERENCES

[1] Bitzer, T. (1998). Honeycomb Technology, vol. 1, Springer us.
[2] Yan, L. Kasal, B. and Huang, L.(2016). A review of recent research on the use of cellulosic fibres, their fibre fabric reinforced cementitious, geo-polymer and polymer composites in civil engineering. *Composites Part B: Engineering*, 92, pp.194-132. https://doi.org/10.1016/j.compositesb.2016.02.002.
[3] Vinson, J. (1999). The Behavior of Sandwich Structures of Isotropic and Composite Materials, 1st Edition éd, New York: CRC Press. https://doi.org/10.1201/9780203737101.
[4] Carlsson L. and Kardomateas, G. (2011). Structural and Failure Mechanics of Sandwich Composites, Solid Mechanics and its Applications 121. Springer. DOI:10.1007/978-1-4020-3225-7.
[5] Monteiro, JG. Sardinha, M. Alves, F. Ribeiro, AR. Reis, L. Deus, AM. Leite, M. and Fatima Vaz, M .(2020). Evaluation of the effect of core lattice topology on the properties of sandwich panels produced by additive manufacturing. J Materials: Design and Applications. 0(0). 1–13. DOI: 10.1177/1464420720958015.

[6] Crameri, S. Stojcevski F. and Mansfield, C. U. (2023). An Experimental Investigation of the Mechanical Performance of EPS Foam Core Sandwich Composites Used in Surfboard Design, Polymers. 15(12):2703. DOI:10.3390/polym15122703.
[7] Huang, P. Gao, Q. Su, X. Feng, Z. Sun, X. and Guoyin, Z. (2008). Effect of core density on the three-point bending performance of aluminum foam sandwich panels. *Materials*. 16(22),7091. DOI:10.3390/ma16227091.
[8] Grosse, C. and Ohtsu, M. Acoustic Emission Testing, Berlin: Springer. DOIhttps://doi.org/10.1007/978-3-540-69972-9.
[9] Saeedifar, M. Fotouhi, Najafabadi, M. A. and Toudeshky, H. H. (2015).Prediction of delamination growth in laminated composites using acoustic emission and Cohesive Zone Modeling techniques. *Composite Structures,*124, pp. 120-127. DOI:10.1016/j.compstruct.2015.01.003.
[10] Fotouhi, M. Saeedifar, M. Sadeghi, S. Najafabadi, M. A. and Minak, G. (2015). Investigation of the damage mechanisms for mode I delamination growth in foam core sandwich composites using acoustic emission. *Structural Health Monitoring*, 14(3), pp. 265–280. DOI:10.1177/1475921714568403.
[11] Assarar, M. Bentahar, M. El Mahi, A. and El Guerjouma, R. (2015). Monitoring of damage mechanisms in sandwich composite materials using acoustic emission. International Journal of Damage Mechanics. 24(6), pp. 787–804. DOI:10.1177/1056789514553134.
[12] Pyrzowski, Ł. Knak, M. and Rucka, M. (2023). Failure characterisation of sandwich beams using integrated acoustic emission and digital image correlation techniques. Composite Structures 322, 117361. DOI: 10.1016/j.compstruct.2023.117361.
[13] Ben Ammar, I. Karra, C. El Mahi, A. El Guerjouma, R. and Haddar, M.(2014). Mechanical behavior and acoustic emission technique for detecting damage in sandwich structures. Applied Acoustics 86, pp. 106–117. DOI:10.1016/j.apacoust.2014.04.016.
[14] Leone Jr, F. A. Ozevin, D. Awerbuch, J. and Tan, T.-M.(2013). Detecting and locating damage initiation and progression in full-scale sandwich composite fuselage panels using acoustic emission. Journal of Composite Materials, 47(13):1643-1664. DOI:10.1177/0021998312450306.
[15] BENHAMADI, G.(2024). SARL HODNA METAL . Available: https://www.hodnametal.dz/index.html.